ACS SyntheticBiology

Letter

pubs.acs.org/synthbio

Real-Time mRNA Measurement during an *in Vitro* Transcription and Translation Reaction Using Binary Probes

Henrike Niederholtmeyer, Ling Xu, and Sebastian J. Maerkl*

School of Engineering, Institute of Bioengineering, École Polytechnique Fédérale de Lausanne, 1015 Lausanne, Switzerland

Supporting Information

ABSTRACT: *In vitro* transcription and translation reactions have become popular for a bottom-up approach to synthetic biology. Concentrations of the mRNA intermediate are rarely determined, although knowledge of synthesis and degradation rates could facilitate rational engineering of *in vitro* systems. We designed binary probes to measure mRNA dynamics during cell-free protein synthesis by fluorescence resonance energy transfer. We tested different mRNA variants and show that the location and sequence environment of the probe target sites are important parameters for probe association kinetics and output signal. Best suited for sensitive real-time quantitation of mRNA was a target site located in the 3′ untranslated region, which we designed to reduce secondary structure. We used this probe−target pair to refine our knowledge of mRNA dynamics in the commercially available PURE cell-free protein synthesis system and characterized the effect of TetR repressor on mRNA synthesis rates from a T7 promoter.

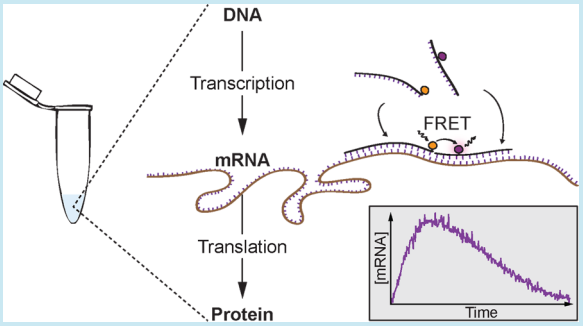

KEYWORDS: *binary probes, FRET, cell-free protein synthesis, in vitro synthetic biology, transcription, mRNA dynamics*

In vitro transcription and translation (ITT) reactions have been widely used and optimized for protein synthesis and screening purposes.[1,2] More recently, those *in vitro* systems have become popular for a bottom-up approach to synthetic biology.[3] Fundamental molecular processes of life were reconstituted *in vitro*, such as the *Escherichia coli* translation machinery from purified components[4] and the *E. coli* RNA polymerase holoenzyme, which was synthesized by adding the DNA templates for the subunits of the enzyme complex into an ITT reaction.[5] Examples for structural self-organization that could be reconstituted in ITT reactions programmed with DNA templates include the synthesis and assembly of the T7 bacteriophage,[6] the self-assembly of cytoskeletal structures in liposomes[7] and emulating embryonic pattern formation.[8] The dynamics and behavior of synthetic gene networks have also been studied in ITT reactions. Multistage cascades, where the gene product of one stage is the input for the next stage, AND gates, and negative feedback loops have been assembled.[3,9−11] All genetic regulators, activators, and repressors employed in these genetic networks acted on the initiation of mRNA synthesis. Furthermore, Shin and Noireaux have established a method to increase mRNA turnover and propose that active mRNA inactivation might facilitate the engineering of informational processes.[12] Despite their focus on regulation of mRNA synthesis and mRNA degradation, these studies only used reporter protein production as their readout. To rationally assemble and characterize *in vitro* genetic networks, it would be helpful to directly quantitate mRNA dynamics and synthesis rates. After all, it is this intermediate that regulation acts upon most often and whose concentration determines protein output, often in a nonlinear fashion as the translation machinery becomes saturated at high concentrations of mRNA.[3]

RNA concentrations can be determined by different techniques *in vivo* and *in vitro*. Potential real-time methods that can detect a specific mRNA employ fluorophores that bind to a region of the mRNA of interest, which changes their emission properties. Examples include "spinach"[13] and oligonucleotide probes like molecular beacons and binary probes.[14,15] Binary probes consist of two DNA oligonucleotides that hybridize to adjacent locations on a target sequence. Each carries a fluorophore of a fluorescence resonance energy transfer (FRET) donor−acceptor pair. When both probes are bound to the target sequence, the fluorophores are brought in close proximity so that FRET can occur. This technique has been used to measure mRNA synthesis during *in vitro* transcription.[16] Models of the transcription and translation processes during GFP synthesis were important steps toward a more quantitative understanding of the dynamics of protein synthesis in cell-free systems.[17,18] These studies also measured mRNA levels over time to take into account synthesis and degradation of mRNA for their models. Stögbauer et al.[18] used a molecular beacon, which bound to a sequence in the GFP coding region on the mRNA.

In this work we designed binary probes, which we tested in combination with different mRNA target designs in order to derive a probe−target pair that allows sensitive real-time

Received: October 3, 2012
Published: December 19, 2012

quantitation in ITT reactions and could be used for other genes without the need for sequence redesign. We demonstrate the value of the probes as a tool for *in vitro* synthetic biology by refining our understanding of RNA dynamics in the PURE ITT system[4] and measuring the effect of the TetR repressor on mRNA synthesis from a $T7_{tet}$ promoter.

We decided to place the probe target site, the nucleotide sequence to which the binary probes bind, outside of the protein coding region, either in the 5′ or 3′ untranslated region (UTR), in order to avoid interference between probe binding and translating ribosomes. This has the additional advantage that the same probe−target combination could be used for other genes without requiring a different set of costly FRET probes and reoptimization of the target sequence. Similar to previous probe designs,[16,19] we chose a sequence of 30 bp as the target for the two probes, which consisted of 15 bp each. We chose Cy3 and Cy5 fluorophores as our FRET pair, with a spacing of 4 nucleotides, or about 1.65 nm, for optimal FRET efficiency[14] (Figure 1).

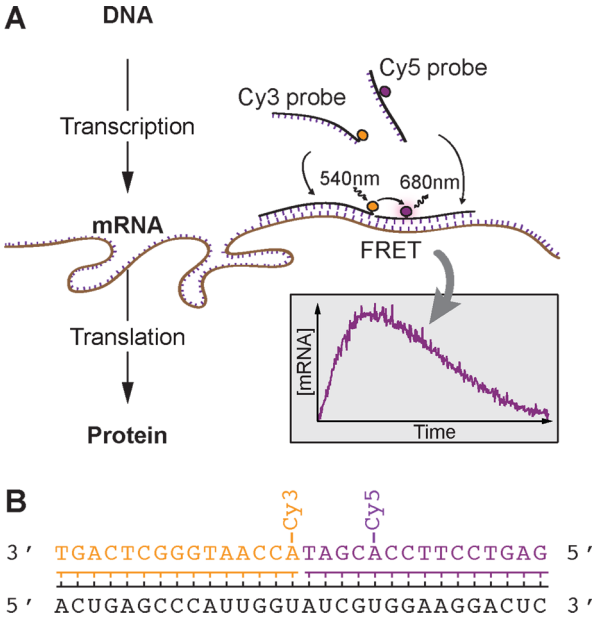

Figure 1. Design of the binary probes and their target sequence. (A) Real-time measurement of mRNA during *in vitro* transcription and translation. mRNA with the target site for the binary probes and the coding region for the protein is produced from a DNA template. The binary probes carrying either a Cy3 or Cy5 fluorophore are present in the ITT mix and hybridize to the RNA. This brings the donor and acceptor fluorophores into close proximity so that FRET can occur. The FRET fluorescence allows quantification of mRNA concentration over time. (B) Sequences of the RNA target (black) and the bound probes with positions of the fluorophores.

We found that the sequence environment of the target site on the mRNA has a strong influence on the observed FRET signal. We thus synthesized different mRNAs *in vitro*, purified them, and compared binding of the binary probes to identical target concentrations. In the different mRNAs tested, the probe target site was placed either in the 5′ or the 3′ UTR (Figure 2A). We tested one mRNA with the target site in the 5′ UTR and three mRNAs with the target site in the 3′ UTR. Those differed in the distance of the target site to the end of the protein coding region (3′ target version 1 compared to versions 2 and 3) and the stability of the secondary structure that could be formed by the nucleotides surrounding the target sequence, which was minimized in version 3 by adding stretches of adenines around the target site (see Supporting Information Figure S10 and Table S1).

We observed a stable FRET signal over 12h when the probes were added to a DNA target in buffer (Figure 2B), showing that no photobleaching occurred under the imaging conditions employed. All mRNAs, except for the negative control without a target sequence, produced measurable FRET signals and EGFP protein, when added to ITT mix (Figure 2D). The binding kinetics and the final FRET signals differed considerably for the target variants tested in both buffer (Figure 2B) and ITT mix (Figure 2C). When the target site was located on mRNA, hybridization of the probes was slower than to the DNA target. The 5′ UTR target gave rise to the slowest binding kinetics and lowest FRET signal. The mRNAs with the target site in the 3′ UTR exhibited faster association kinetics and higher FRET signals, indicating that mRNA secondary structure and target site location are important parameters (see Supporting Information Table S1). The fastest binding kinetics and highest FRET signal was observed for the 3′ UTR with the sequence that was specifically optimized to reduce secondary structure in the nucleotides surrounding the 30 bp target sequence. It was our goal to have a sensitive real-time measurement of mRNA during *in vitro* protein synthesis, so for all subsequent experiments, we used the 3′ UTR version 3. In addition, this 3′ UTR also increased protein production probably by altering the secondary structure of the mRNA (Figure 2D).

During synthesis of mRNA from the different DNA templates (Figure 2A), the 3′ target 3 also gave rise to the highest FRET signal when tested in a transcription reaction (Supporting Information Figure S1) as well as in an ITT reaction (Supporting Information Figure S2). Although different concentrations of mRNA were synthesized, these differences could not explain the differences in signal, which shows that during synthesis of mRNA, probe hybridization kinetics are important for sensitivity. When identical concentrations of purified mRNA were added into an ITT reaction, we observed the same dependence of hybridization kinetics and FRET signal on target site position as in buffer, but here the FRET signal declined exponentially after reaching a peak at about 20 min (Figure 2C). We attributed this decline to mRNA degradation. We verified by qRT-PCR that mRNA degradation was indeed occurring at a comparable rate as determined by our FRET probes (Figure 3). Degradation of mRNA follows first order kinetics.[12,17] This exponential decay can be described by the following function:

$$m(t) = m_0 e^{-\deg_m t} \quad (1)$$

where m_0 is the initial mRNA concentration and $\deg_m$ the mRNA degradation rate.

Known amounts of mRNA were added to ITT mix containing an excess amount of binary probes (1 μM). The decreasing FRET signals of different initial mRNA concentrations (250−900 nM, starting at 40 min, see Supporting Information Figure S3) were fitted to eq 1, and the RNA degradation rate was determined to be 0.0085 ± 0.0019 min^{-1}, which is 10-fold greater than the value reported for the PURE system in a previous study,[18] where mRNA degradation had not been observed experimentally but was determined by fitting a model with eight free parameters to the experimental data.

dx.doi.org/10.1021/sb300104f | *ACS Synth. Biol.* 2013, 2, 411−417

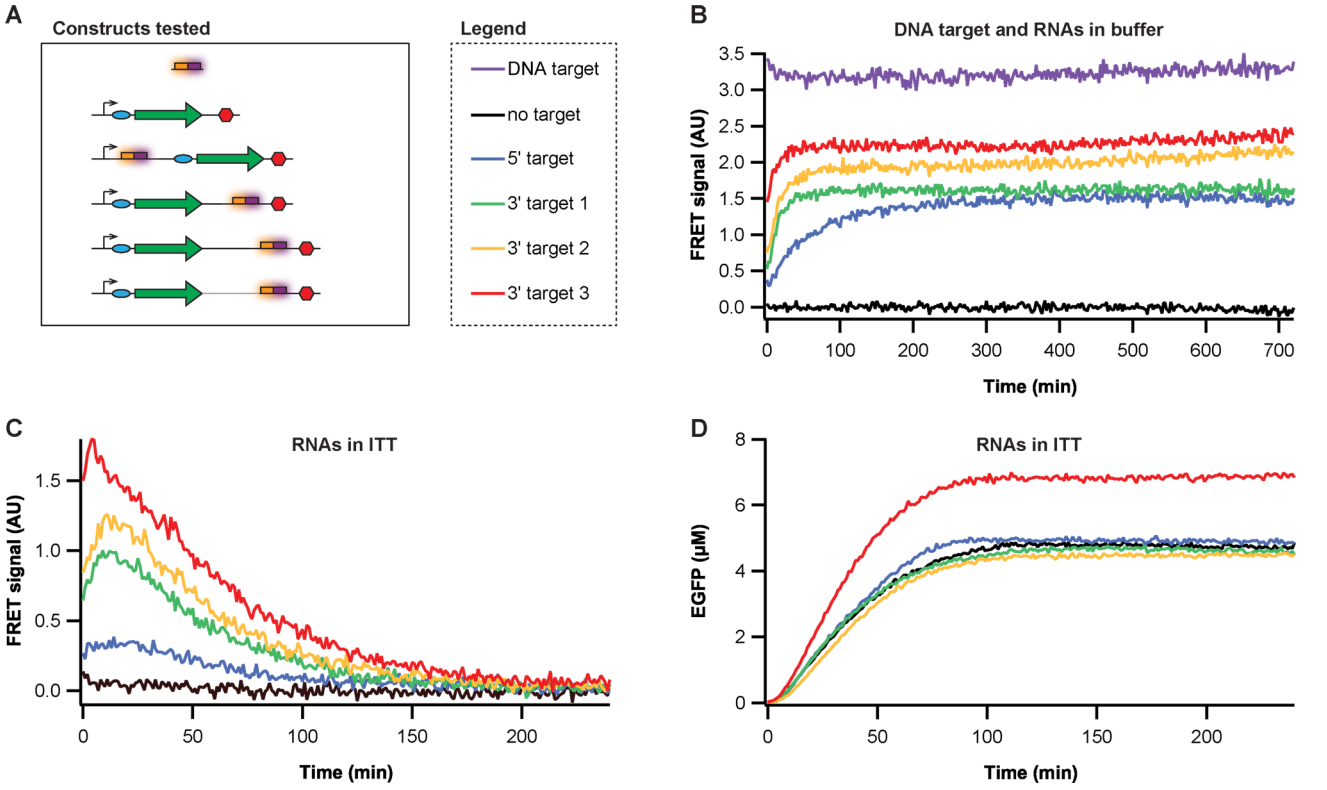

Figure 2. Effect of the sequence environment of the target site on hybridization kinetics and FRET signal. (A) Schematics of the different DNA templates, from which the mRNA that were compared for probe binding were synthesized. The DNA target was the 30 bp single stranded complementary sequence to the probes. The mRNAs were produced by *in vitro* transcription with T7 RNA polymerase (the black arrow depicts the T7 promoter and the red hexagon the T7 terminator). All mRNAs contained the same EGFP coding region (green arrow) and ribosomal binding site (blue circle). They differed in the position and the sequence around the target site (orange and purple box) located in the 5′ or 3′ UTR. (B,C) Hybridization of the binary probes (each at 1 μM) to DNA or mRNA target (all at 480nM) in buffer (B) or ITT mix (C). FRET signal was calculated by normalizing the FRET fluorescence to the Cy5 fluorescence and subtracting the FRET background from a reaction containing no RNA or DNA (see Methods for details). (D) EGFP concentration produced by the reactions in (C).

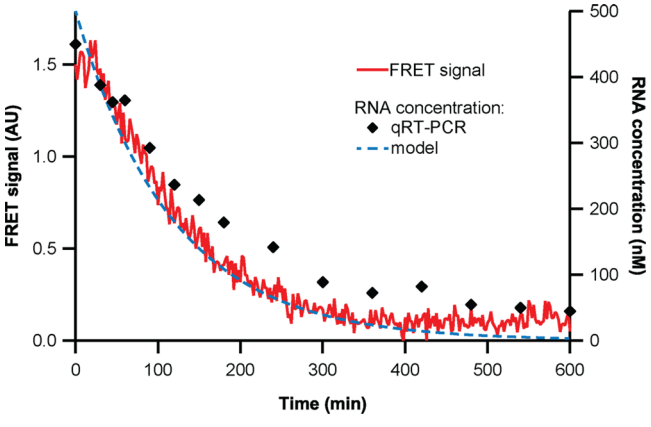

Figure 3. Degradation of mRNA in the PURE ITT mix. Degradation of 500 nM mRNA in ITT mix as observed by qRT-PCR and FRET signal. The experimental results are compared to the predicted RNA concentration for a degradation rate of 0.0085 min^{-1}.

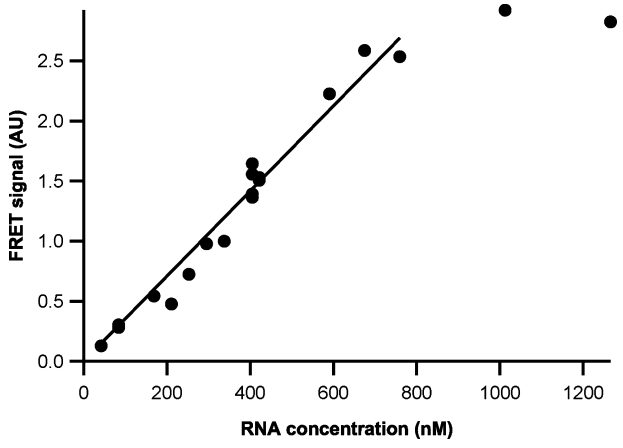

Figure 4. Calibration of the FRET signal to mRNA concentration. The peak FRET signal around 20 min (average of signal between 10 and 30 min) was plotted against the RNA concentration at 20 min, which was calculated from the known initial mRNA concentration using the determined degradation rate. For mRNA concentrations smaller than probe concentration (1 μM) the FRET signal increased linearly with a slope of 0.0035 nM^{-1}.

In order to calibrate the FRET signal to mRNA concentration, we used the peak FRET signal of different mRNA concentrations (average of signal from 10 to 30 min) and plotted this against the mRNA concentration at 20 min, which was calculated from the known initial concentration and the RNA degradation rate. The FRET signal increased linearly with mRNA concentration until mRNA concentration exceeded probe concentration (Figure 4). At a probe concentration of 1 μM, we could detect mRNA concentrations ranging from 50 to 900 nM. At mRNA concentrations below 50 nM, the signal-to-noise ratio was too low to allow a reliable quantitation under our experimental conditions.

dx.doi.org/10.1021/sb300104f | *ACS Synth. Biol.* 2013, 2, 411–417

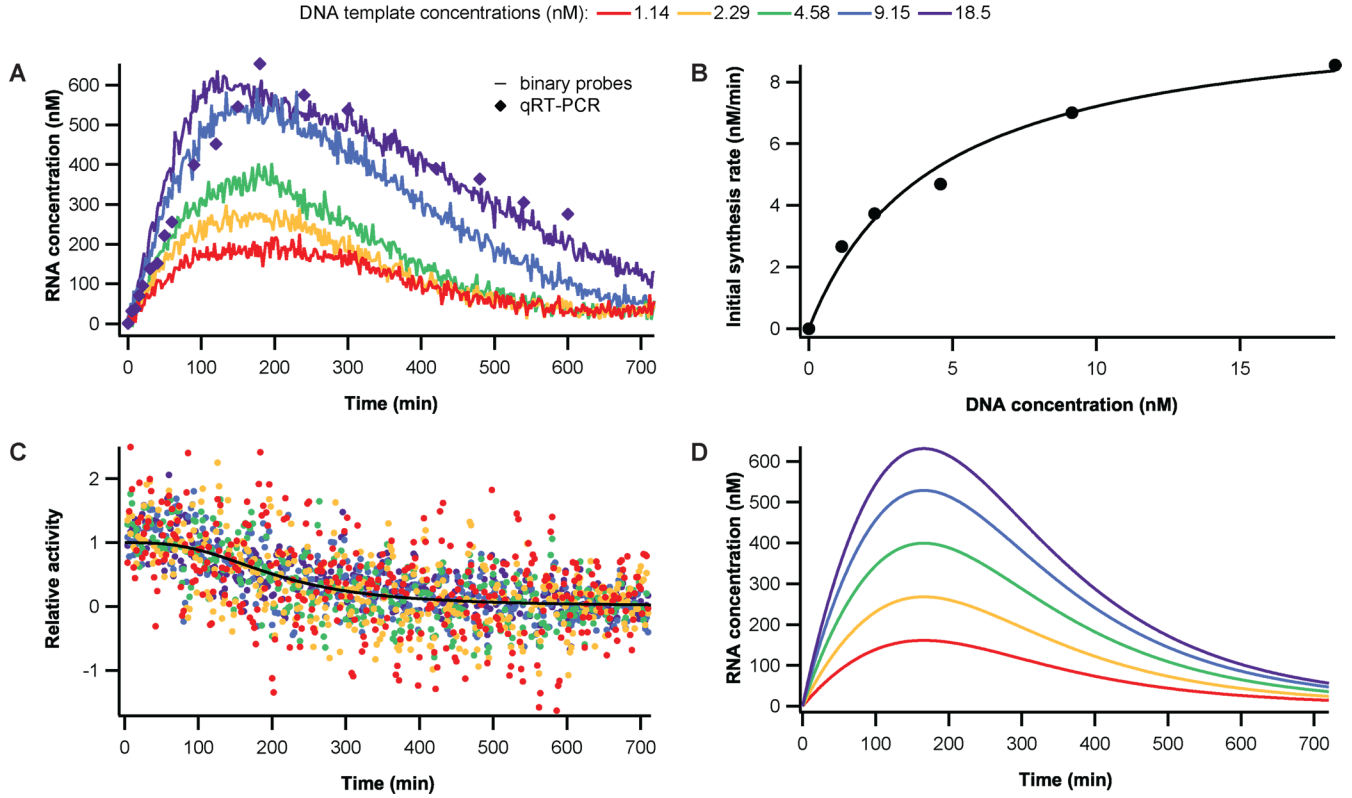

Figure 5. RNA synthesis from different DNA template concentrations during ITT. (A) RNA concentrations during synthesis from different template concentrations in ITT, measured by binary probes and qRT-PCR. (B) Initial mRNA synthesis rates for different DNA template concentrations. Initial rates were determined from the first 100 min of synthesis assuming no decline of transcriptional activity. (C) Relative transcriptional activity over time during synthesis from different DNA template concentrations. Relative activity was determined with eq 7 from the concentration change during a time increment of 6 min. To reduce the noise we used the average of 3 measurements (corresponding to 6 min) around each time point. With the known mRNA degradation and initial synthesis rate we could calculate what fraction of initial activity was left at each time point. The black line is the Hill function (eq 8), which was used to fit the results (see Supporting Information Figure S6). (D) Results of our model of mRNA dynamics in ITT at different DNA template concentrations. The model took into account mRNA degradation and a transcription rate, which is dependent on the DNA template concentration (B) and time (C).

Using the calibration of the FRET signal, we could quantitate mRNA synthesis from a DNA template. The mRNA synthesis rate depended on the DNA template concentration used in the ITT reaction (Figure 5A). Although the mRNA concentrations differed more than 3-fold over the range of DNA template concentration tested, the effect on EGFP concentration was low, showing that the translation machinery became saturated above 200 nM of mRNA (see Supporting Information Figures S3B and S4B). The mRNA measurement determined from the FRET signal was confirmed by qRT-PCR for the highest DNA template concentration (Figure 5A).

The change in mRNA concentration, m, can be described by the following differential equation:

$$m'(t) = \mathrm{syn}(d) - \deg_m m(t) \tag{2}$$

The transcriptional activity, $\mathrm{syn}(d)$, is a function of the DNA concentration, d. The degradation rate of mRNA, $\deg_m$, we previously determined. With $m(0) = 0$, the solution of eq 2 for a given DNA template concentration is as follows:

$$m(t) = \frac{\mathrm{syn}(d)}{\deg_m}\left(1 - e^{-\deg_m t}\right) \tag{3}$$

To determine initial transcription rates, the mRNA concentrations of the different DNA template concentrations during the first 100 min of the reaction were fitted to eq 3 (Supporting Information Figure S4A) and plotted against DNA concentration (Figure 5B). Transcription can be described by Michaelis–Menten kinetics:

$$\mathrm{syn}(d) = \frac{v_{\max} d}{K_{\mathrm{TS}} + d} \tag{4}$$

By fitting eq 4, the maximum transcription rate, $v_{\max}$, was determined to be 10.4 nM/min, and the DNA concentration for half-maximal transcription rate, K_{TS}, was 4.4 nM (Figure 5B). Both values were in good agreement with values reported by Stögbauer et al. using the same ITT mix.[18]

To be able to describe the complete reaction, we have to take into account a decrease of transcriptional activity because the process consumes substrates and enzymes can degrade. If there was no decrease of transcriptional activity, the mRNA concentration would reach a steady state when mRNA synthesis and degradation are balanced (Supporting Information Figure S5). The fact that mRNA concentration decreases after reaching a maximum at about 2–3 h suggests that the transcriptional activity decreases. In contrast to Stögbauer et al.,[18] we did not observe a clear dependence of the time when RNA synthesis ceases on the DNA concentration (Figure 5A). At this point, we did not want to make any assumptions on the mode by which transcriptional activity decreases, so we

dx.doi.org/10.1021/sb300104f | ACS Synth. Biol. 2013, 2, 411–417

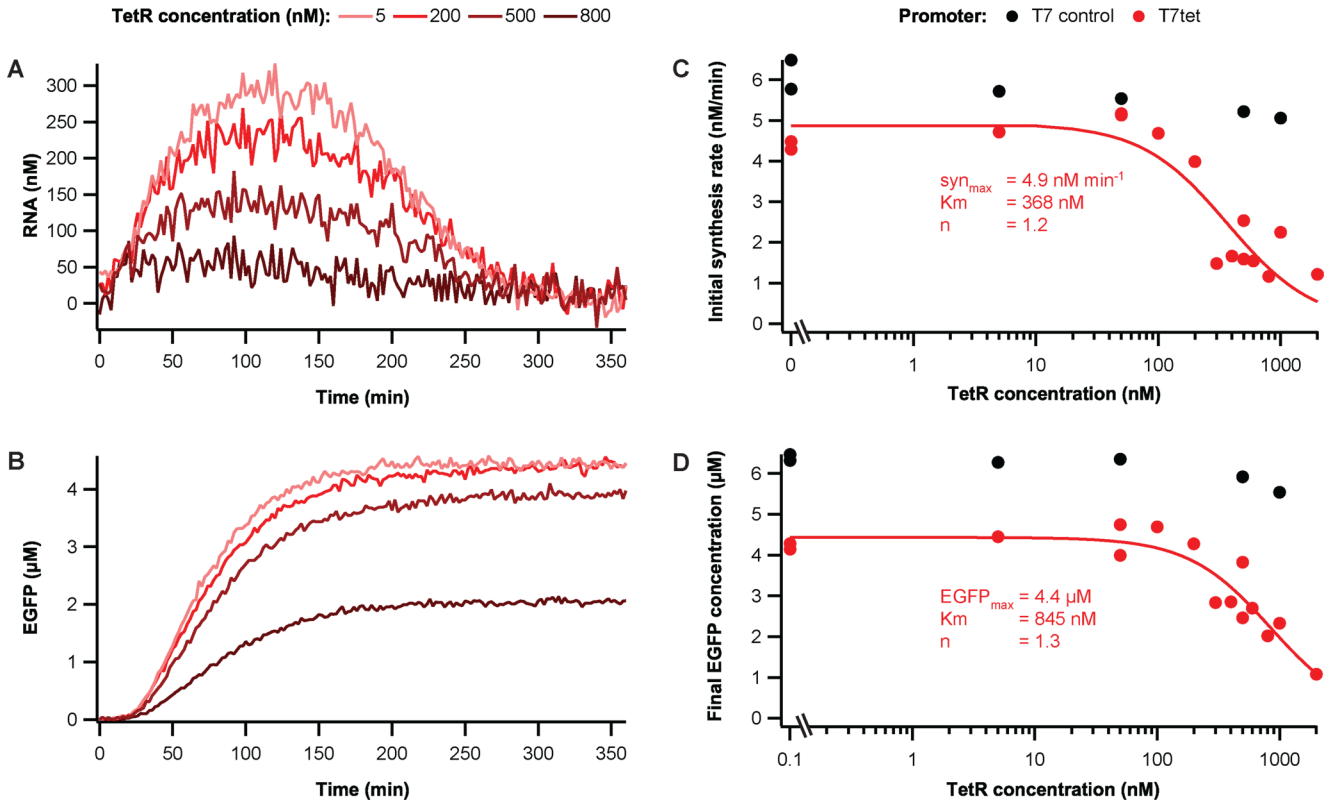

Figure 6. Repression of transcription from the $T7_{tet}$ promoter by TetR. Examples of mRNA (A) and EGFP (B) synthesis driven by the $T7_{tet}$ promoter at different concentrations of TetR repressor. DNA template concentration was 10 nM. (C) Initial mRNA synthesis rates versus TetR concentration for the $T7_{tet}$ promoter and the constitutive T7 promoter control. (D) End point EGFP concentrations for $T7_{tet}$ and constitutive T7 promoter at different TetR concentrations. The RNA synthesis rates and final EGFP concentrations of the repressed promoter were fitted to a Hill function (eq 9) to determine maximal activity, concentration of TetR for half-maximal activity and Hill coefficient.

introduced the relative activity, act(t), as the fraction of initial transcriptional activity at time t.

$$m'(t) = \mathrm{act}(t)\mathrm{syn}(d) - \deg_m m(t) \tag{5}$$

Using Euler's method, mRNA concentration over time can be approximated with the following:

$$m(t + \Delta t) = m(t) + (\mathrm{act}(t)\mathrm{syn}(d) - \deg_m m(t))\Delta t \tag{6}$$

$$\mathrm{act}(t) = \frac{m(t + \Delta t) - m(t) + \deg_m m(t)\Delta t}{\Delta t \mathrm{syn}(d)} \tag{7}$$

Using eq 7 and the experimental results for mRNA concentration, we calculated the relative transcriptional activity comparing two time points with a fixed time increment of Δt over the course of the ITT reaction (Figure 5C). For all DNA template concentrations, the relative transcriptional activity followed a sigmoidal curve. For the first hour it remained at its initial rate and then decreased to 0 after about 8 h (Figure 5C, Supporting Information Figure S6). Interestingly, the transcription rate started to decrease when EGFP synthesis started to plateau. It has been shown that a decrease in energy charge caused by the hydrolysis of nucleoside tri- and diphosphates is the limiting factor for cell-free protein synthesis reactions.[3,4] Translation is the main contributor to this decrease in energy charge.[20] Transcription, however, also requires nucleoside triphosphates, which could explain why protein and mRNA synthesis cease at the same time. The relative mRNA synthesis activities were fitted by a Hill function:

$$\mathrm{act}(t) = 1 - \frac{1}{1 + \left(\frac{t_{half}}{t}\right)^n} \tag{8}$$

For neither the time of half-maximal activity, t_{half}, nor the Hill coefficient, n, which determines the steepness of the activity decline, could a dependence on DNA concentration be observed (Supporting Information Figure S6). The average of t_{half} was 203 ± 13 min and 2.9 ± 0.7 for n (black line in Figure 5C). With this, eq 5 could predict mRNA concentration over the complete reaction time of 12 h for different DNA template concentrations (Figure 5D). We also show that the decrease in transcriptional activity could not be explained by a degradation of the DNA templates, which degrade at a much slower rate (Supporting Information Figure S7).

Regulators in genetic networks often act by modulating transcription. A number of transcriptional activators and repressors have been used to build *in vitro* networks.[3,9−11] In ITT reactions their effect has, to our knowledge, only been studied as output of a reporter protein product. For a rational design of *in vitro* networks, it would however be useful to study the effect on mRNA synthesis directly. We applied our method of real-time mRNA measurement to the repression of a T7 promoter by TetR. Instead of the standard T7 promoter used to drive expression in the previous experiments, the $T7_{tet}$ promoter included the TetR operator sequence downstream of the T7 promoter. This promoter had been previously shown to be repressible by TetR in *Leishmania*[21] (see Supporting Information Figure S10). Purified TetR protein was added at different concentrations to the ITT reaction, and a dependence

dx.doi.org/10.1021/sb300104f | *ACS Synth. Biol.* 2013, 2, 411−417

of mRNA synthesis rate and EGFP output on TetR concentration was observed (Figure 6 and Supporting Information Figure S8). 1000 nM of TetR inhibited transcription almost 5-fold, while the control reactions with the standard T7 promoter without a TetR binding site remained unaffected (Figure 6C). The maximum transcription rate syn_{max} (4.9 nM/min), the TetR concentration for half-maximal repression (368 nM), *Km*, and the Hill coefficient (1.2) were determined by fitting a Hill function (Figure 6C):

$$\mathrm{syn}([\mathrm{TetR}]) = \frac{\mathrm{syn}_{max} Km^n}{Km^n + [\mathrm{TetR}]^n} \quad (9)$$

The *Km* we observed is substantially higher than the affinity of TetR to its operator, which was determined to be 5.6 nM.[22] This discrepancy can be explained by the fact that repressor and polymerase do not exclude each other from the promoter, as has been found for inhibition of T7 RNA polymerase by the *lac* repressor bound at a similar distance downstream of the promoter.[23] Operator placement in respect to the T7 promoter is important for the repression characteristics,[24,25] and it seems that there is a trade-off between maximal expression strength and efficient repression depending on the distance of the operator to the transcriptional start site.[10] With the first base of the *tet* operator at +9 relative to the T7 promoter, we measured an intermediate *Km* of about 370 nM in respect to the values determined by Karig et al.,[10] which were 73 nM for the operator starting at +4 and 3000 nM for the operator starting at +10. We would like to stress however that Karig et al. determined repression via protein output, which might have masked a repression of transcription rate in the case of the latter, stronger promoter due to saturation of the translational machinery with mRNA. We observed this effect for EGFP output (Figure 5D), where half-maximal repression is obtained at a higher TetR concentration (845 nM).

For a thorough characterization of genetic parts and devices in ITT reactions, it will be useful to determine transcription rates directly and in real-time. In this regard, the 3′ UTR target−binary probe pair we described in this work will be a useful tool for *in vitro* synthetic biology to quantitate mRNA concentrations in ITT reactions. Our probe−target pair has been optimized for fast binding kinetics to provide sensitive real-time measurements and can be used for other genes of interest. It could also be useful for *in vitro* transcriptional circuits, where a number of different RNA molecules are synthesized.[26] We applied the method to refine our knowledge of mRNA dynamics in the PURE system, where we found that mRNA degradation plays a more important role than had been previously suggested,[18] and we characterized the repression of a $T7_{tet}$ promoter[21] by TetR in the same cell-free protein synthesis kit.

METHODS

DNA Linear Template Preparation and Sequences. DNA templates for ITT or *in vitro* RNA synthesis reactions were prepared by two-step PCR.[27] The EGFP coding region was amplified from pKT127[28] with gene specific primers, which also introduced a strong ribosomal binding site. T7 promoter and terminator, as well as the respective 5′ and 3′ UTRs, which contained the target sites, were added in the second step of the PCR by the 3′ and 5′ extension primers (see Supporting Information Table S2). PCR products were purified before use, and concentrations were determined with a Nanodrop spectrophotometer. Oligonucleotides used as primers and the binary probes were purchased from IDT DNA. The binary probes had the following sequences: 5′-/Cy3/ACCAATGGGCTCAGT-3′ and 5′-GAGTCCTTCC/Cy5/ACGAT-3′.

Reaction Setup and RNA and EGFP Measurements. RNA and DNA targets were tested in Buffer 4 (New England Biolabs) supplemented with 200 μg/mL BSA and 1 μM probes. For ITT reactions, the commercial kit PURExpress (New England Biolabs) was used following the manufacturers instructions. Reactions were supplemented with Protector RNase Inhibitor (Roche), 1 μM of each probe, DNA or mRNA and TetR repressor (Imgen Biosciences) at the indicated concentrations. Reaction volume was 5 μL, which was centrifuged to the bottom of wells in optical 384-well polystyrene plates (Nunc) and covered with 35 μL of Chill-Out Liquid wax (Biorad) to avoid evaporation. Reactions were performed at 37 °C in a Biotek SynergyMx plate reader at 37 °C without shaking. Every 2 min for 12 h EGFP fluorescence (excitation 485 ± 9 nm, emission 515 ± 9 nm at a sensitivity of 70), Cy5 fluorescence (650 ± 9 nm, 680 ± 9 nm, sensitivity 100) and Cy3/Cy5 FRET fluorescence (540 ± 20 nm, 680 ± 20 nm, sensitivity 100) were measured. Fluorescence of technical repeats varied substantially because of the small reaction volume. We found that we could significantly reduce this variability by normalizing to the Cy5 fluorescence, which is unaffected from probe binding. EGFP and FRET signals were determined by dividing with Cy5 fluorescence of the respective well. For FRET signals, we additionally subtracted the background fluorescence of a reaction that contained water instead of DNA or mRNA template over time. EGFP signal was calibrated to known concentrations of purified protein (BioVison) (Supporting Information Figure S9).

Preparation of Pure mRNA and qRT-PCR. RNA was prepared with the MEGAscript T7 kit (Ambion) and purified with the MEGAclear kit (Ambion) following the manufacturers instructions. Concentrations were determined spectrophotometrically. As a control, mRNA concentrations during ITT reactions were measured by qRT-PCR. For this, 1 μL samples were taken at different time points from a tube containing ITT mix at 37 °C and diluted 50-fold in H_2O. These samples were stored at −80 °C until used. If necessary, a DNase treatment was performed using the TURBO DNA-free kit (Life Technologies). Afterward the samples were further diluted to a final dilution of 1:10 000. Two microliters of sample were analyzed in 10 μL reactions of the Power SYBR Green RNA-to-CT 1-Step kit (Life Technologies) in the 7500 Fast Real-Time PCR System (Applied Biosystems). Primers amplified a region of the EGFP gene (see Supporting Information Table S2) and were used at 0.6 μM for the forward and at 0.3 μM for the reverse primer. These conditions resulted in PCR efficiencies between 96 and 98%. Concentrations were determined from a standard curve of dilutions of purified mRNA synthesized from the T7-EGFP 3′ target version 3 template in a range from 0.3 to 36.3 pM mRNA per PCR reaction.

ASSOCIATED CONTENT

Supporting Information

Supporting Tables S1−2 and Supporting Figures S1−10. This information is available free of charge via the Internet at http://pubs.acs.org/.

AUTHOR INFORMATION

Corresponding Author

*E-mail: sebastian.maerkl@epfl.ch. Tel: +41 21 6937835.

Author Contributions

H.N., L.X., and S.J.M. designed the experiments. H.N. and L.X. performed the experiments. H.N. and S.J.M. analyzed the data and wrote the manuscript.

Notes

The authors declare no competing financial interest.

ACKNOWLEDGMENTS

We thank Marcel Geertz for helpful discussions. This work was supported by EPFL and the EPFL summer research program (L.X.).

REFERENCES

(1) Woodrow, K. A., and Swartz, J. R. (2007) A sequential expression system for high-throughput functional genomic analysis. *Proteomics 7*, 3870−3879.

(2) Spirin, A. S. (2004) High-throughput cell-free systems for synthesis of functionally active proteins. *Trends Biotechnol. 22*, 538−545.

(3) Noireaux, V., Bar-Ziv, R., and Libchaber, A. (2003) Principles of cell-free genetic circuit assembly. *Proc. Natl. Acad. Sci. U. S. A. 100*, 12672−12677.

(4) Shimizu, Y., Inoue, A., Tomari, Y., Suzuki, T., Yokogawa, T., Nishikawa, K., and Ueda, T. (2001) Cell-free translation reconstituted with purified components. *Nat. Biotechnol. 19*, 751−755.

(5) Asahara, H., and Chong, S. (2010) In vitro genetic reconstruction of bacterial transcription initiation by coupled synthesis and detection of RNA polymerase holoenzyme. *Nucleic Acids Res. 38*, e141.

(6) Shin, J., Jardine, P., and Noireaux, V. (2012) Genome replication, synthesis, and assembly of the bacteriophage T7 in a single cell-free reaction. *ACS Synth. Biol. 1*, 408−413.

(7) Maeda, Y. T., Nakadai, T., Shin, J., Uryu, K., Noireaux, V., and Libchaber, A. (2011) Assembly of MreB filaments on liposome membranes: a synthetic biology approach. *ACS Synth. Biol. 1*, 53−59.

(8) Isalan, M., Lemerle, C., and Serrano, L. (2005) Engineering gene networks to emulate *Drosophila* embryonic pattern formation. *PLoS Biol. 3*, e64.

(9) Ishikawa, K., Sato, K., Shima, Y., Urabe, I., and Yomo, T. (2004) Expression of a cascading genetic network within liposomes. *FEBS Lett. 576*, 387−390.

(10) Karig, D. K., Iyer, S., Simpson, M. L., and Doktycz, M. J. (2012) Expression optimization and synthetic gene networks in cell-free systems. *Nucleic Acids Res. 40*, 3763−3774.

(11) Shin, J., and Noireaux, V. (2012) An *E. coli* cell-free expression toolbox: application to synthetic gene circuits and artificial cells. *ACS Synth. Biol. 1*, 29−41.

(12) Shin, J., and Noireaux, V. (2010) Study of messenger RNA inactivation and protein degradation in an *Escherichia coli* cell-free expression system. *J. Biol. Eng. 4*, 9.

(13) Paige, J. S., Wu, K. Y., and Jaffrey, S. R. (2011) RNA mimics of green fluorescent protein. *Science 333*, 642−646.

(14) Didenko, V. V. (2001) DNA probes using fluorescence resonance energy transfer (FRET): designs and applications. *Biotechniques 31*, 1106−1121.

(15) Marras, S. A. E., Tyagi, S., and Kramer, F. R. (2006) Real-time assays with molecular beacons and other fluorescent nucleic acid hybridization probes. *Clin. Chim. Acta 363*, 48−60.

(16) Sei-Iida, Y., Koshimoto, H., Kondo, S., and Tsuji, A. (2000) Real-time monitoring of *in vitro* transcriptional RNA synthesis using fluorescence resonance energy transfer. *Nucleic Acids Res. 28*, e59.

(17) Karzbrun, E., Shin, J., Bar-Ziv, R. H., and Noireaux, V. (2011) Coarse-grained dynamics of protein synthesis in a cell-free system. *Phys. Rev. Lett. 106*, 48104.

(18) Stögbauer, T., Windhager, L., Zimmer, R., and Rädler, J. O. (2012) Experiment and mathematical modeling of gene expression dynamics in a cell-free system. *Integr. Biol. 4*, 494−501.

(19) Tsourkas, A., Behlke, M. A., Xu, Y., and Bao, G. (2003) Spectroscopic features of dual fluorescence/luminescence resonance energy-transfer molecular beacons. *Anal. Chem. 75*, 3697−3703.

(20) Calhoun, K. A., and Swartz, J. R. (2007) Energy systems for ATP regeneration in cell-free protein synthesis reactions. *Methods Mol. Biol. 375*, 3−17.

(21) Yao, C., Luo, J., Hsiao, C.-H. C., Donelson, J. E., and Wilson, M. E. (2007) *Leishmania chagasi*: a tetracycline-inducible cell line driven by T7 RNA polymerase. *Exp. Parasitol. 116*, 205−213.

(22) Kamionka, A., Bogdanska-Urbaniak, J., Scholz, O., and Hillen, W. (2004) Two mutations in the tetracycline repressor change the inducer anhydrotetracycline to a corepressor. *Nucleic Acids Res. 32*, 842−847.

(23) Lopez, P. J., Guillerez, J., Sousa, R., and Dreyfus, M. (1998) On the mechanism of inhibition of phage T7 RNA polymerase by lac repressor. *J. Mol. Biol. 276*, 861−875.

(24) Dubendorff, J. W., and Studier, F. W. (1991) Controlling basal expression in an inducible T7 expression system by blocking the target T7 promoter with lac repressor. *J. Mol. Biol. 219*, 45−59.

(25) Giordano, T. J., Deuschle, U., Bujard, H., and McAllister, W. T. (1989) Regulation of coliphage T3 and T7 RNA polymerases by the lac repressor-operator system. *Gene 84*, 209−219.

(26) Kim, J., and Winfree, E. (2011) Synthetic *in vitro* transcriptional oscillators. *Mol. Syst. Biol. 7*, 1−15.

(27) Geertz, M., Rockel, S., and Maerkl, S. J. (2012) A high-throughput microfluidic method for generating and characterizing transcription factor mutant libraries. *Methods Mol. Biol. 813*, 107−123.

(28) Sheff, M. A., and Thorn, K. S. (2004) Optimized cassettes for fluorescent protein tagging in *Saccharomyces cerevisiae*. *Yeast 21*, 661−670.